Generated Pattern Current for Photovoltaic Cell and Module Activation:

Defect Stabilization Kinetics via Controlled Carrier Injection

Ibrahim Karakoc

GigaPulse Energy, Turkey | *ibrahim@gigapulse.energy*

PCT/TR2025/051176 | USPTO Appl. No. 19/298,223 | Priority Date: July 23, 2025

Abstract

Photovoltaic (PV) modules exhibit transient performance variations during early operation due to defect activation, trap filling, and recombination center stabilization. This transition — managed through conventional light soaking or constant current injection — typically manifests as a 1–3% efficiency (Δη) loss or shift. Existing literature models activation kinetics as functions of average injection current and temperature. This approach misses the physical mechanism underlying activation: trap capture probability depends not on average current but on the temporal dynamics of carrier density — n(t).

This paper describes the application of the Generated Pattern Current (GPC) paradigm to PV cell and module activation. GPC-based carrier injection applies a parameterized pattern current I(t) instead of constant current, accelerating trap stabilization through three physical mechanisms: (1) enhanced peak carrier density n_peak producing linear capture rate increase, (2) quasi-Fermi level oscillation activating traps at different energy levels sequentially, (3) trap pumping effect by matching pattern frequency to trap emission time constants. These three mechanisms form a mathematical parallel with SEI control physics in battery formation: $dX/dt = K_1 \cdot \Phi\_build(t) - K_2 \cdot \Phi\_harm(t)$. GPC applies the same control philosophy — temporal structure directing interface/defect processes — in both domains.

Keywords: *Generated Pattern Current (GPC), photovoltaic activation, carrier injection, trap stabilization, light-induced degradation (LID), Shockley-Read-Hall, defect kinetics, boron-oxygen complex, quasi-Fermi level*

1. Introduction

1.1 The PV Activation Problem

Every photovoltaic module undergoes an activation period after fabrication [2,3]. During this period, defect states stabilize, carrier recombination centers evolve, and efficiency may temporarily decrease (light-induced degradation — LID) or increase (passivation effects) [4,5,6]. In crystalline silicon modules, the dominant degradation mechanism is the formation of boron-oxygen (B-O) complexes; this process typically causes 1–3% absolute efficiency loss and occurs on a timescale of hours to days [7,8,9].

Conventional activation uses two methods: light soaking or constant electrical current injection. Neither method explicitly controls carrier dynamics. The injected current is constant; carrier density remains approximately steady-state, and trap filling kinetics are confined to an exponential waiting process.

1.2 The Literature Gap

Existing studies model activation through three variables: average injection current (I_avg), temperature (T), and activation time (t). This approach misses the fundamental driver of activation

— the temporal behavior of carrier density n(t). According to Shockley-Read-Hall (SRH) theory [13,14], trap capture rate depends directly on instantaneous carrier density: $R_c = \sigma \cdot v_{th} \cdot n \cdot (N_t - N_{occ})$. Under constant current injection, $n \approx$ constant and $dN_t/dt = k_c \cdot n \cdot (N_{max} - N_t)$ — a saturation curve that starts fast and decelerates exponentially.

The core argument of this paper: Activation ≠ f(I_avg). Activation = f(n(t)). If the temporal structure of carrier density can be controlled, activation kinetics can be accelerated — with the same average energy.

1.3 The GPC Paradigm and PV Application

Generated Pattern Current (GPC) is an electrical control paradigm defined in patent filings PCT/TR2025/051176 and USPTO 19/298,223 [1]. The core principle of GPC: the temporal structure of current is the instruction to the target system — not merely energy. In battery formation (Paper I), this principle was applied as SEI nucleation and growth control [22,23,24]. In this paper, the same principle is applied as carrier injection control in PV cell and module activation. The patent scope explicitly covers this application.

Paper structure: Section 2 covers PV cell physics and carrier dynamics. Section 3 details defect and trap stabilization mechanisms. Section 4 presents the GPC-based carrier injection framework and three physical mechanisms. Section 5 establishes the battery-PV unifying framework. Section 6 defines activation metrics and expected outcomes. Section 7 presents the open validation framework. Section 8 discusses conclusions.

2. PV Cell Physics and Carrier Dynamics

2.1 Cell Electrical Model

A photovoltaic cell can be modeled as an equivalent circuit comprising a photocurrent source, parallel diode, series resistance, and junction capacitance [12,15]:

$$I = I_{ph} - I_D - I_{sh} \quad , \quad I_D = I_0(\exp(V/nV_T) - 1)$$

Including junction capacitance introduces dynamic behavior:

$$C_j \cdot dV/dt = I_{inj} - I_D - I_{sh}$$

This equation shows that the temporal structure of injected current directly affects cell voltage and therefore carrier density. Under constant current injection, $dV/dt \rightarrow 0$ and the system reaches steady state. Under GPC injection, $dV/dt \neq 0$ and carrier density varies with time.

2.2 Carrier Density Dynamics

$$dn/dt = G - R \quad , \quad R = n/\tau$$

where G is the generation rate, R the recombination rate, and τ the carrier lifetime. The carrier transport equation:

$$\partial n/\partial t = D\nabla^2 n - n/\tau + G$$

When carrier density changes rapidly (high dn/dt), diffusion flux develops and carriers spread across a wider volume — making more traps accessible [15,16].

The distinction between steady-state and transient carrier density is critical for understanding why GPC outperforms constant current injection. Under steady-state conditions (constant

current), carrier density reaches an equilibrium value n_ss, and all traps within the corresponding quasi-Fermi level are progressively filled, but traps at deeper energy levels remain inaccessible [12,20]. Under GPC injection, the periodic modulation creates transient peaks where n_peak exceeds n_ss by a factor determined by the pattern amplitude ratio. During these peaks, the quasi-Fermi level temporarily rises, accessing deeper traps that would remain unfilled under constant injection at the same average current.

Furthermore, the spatial distribution of carriers changes under transient conditions. When current drops during the low phase of a GPC pattern, carriers diffuse from regions of high concentration near the surface toward regions of low concentration deeper in the bulk. This diffusion-driven redistribution exposes bulk traps that are geometrically inaccessible under surface-dominated steady-state injection [15,17]. The effective volume participating in the activation process is therefore larger under GPC than under constant current, even when the average current is identical.

3. Defect and Trap Stabilization

3.1 Trap Filling Kinetics

PV activation primarily affects three structures: dangling bonds, impurity complexes, and interface traps [16,19,20]. According to SRH theory [13,14], trap capture rate:

$$R_c = \sigma \cdot v_{th} \cdot n \cdot (N_t - N_{occ})$$

where σ is the capture cross section, v_th the thermal velocity, n the carrier density, N_t the trap density, and N_occ the occupied trap count. From this, clearly: R_c ∝ n.

Trap filling dynamics:

$$dN_{occ}/dt = k_c \cdot n(t) \cdot (N_t - N_{occ}) - k_e \cdot N_{occ}$$

Under constant current, this equation yields standard exponential saturation: N_occ(t) = N_max(1 − exp(−t/τ_trap)). When n(t) becomes time-dependent through GPC, the kinetic structure changes fundamentally.

3.2 Boron-Oxygen Complexes and LID

In crystalline silicon modules, the dominant cause of LID is the formation of boron-oxygen (B-O) complexes [4,5,18]. Performance loss model:

$$\eta(t) = \eta_0 - \Delta\eta \cdot (1 - exp(-t/\tau_{LID}))$$

B-O complex formation and stabilization can be accelerated through carrier injection [9,10,11]. The critical point: the stabilization process depends not only on average injection current but on the temporal profile of carrier density. GPC controls this profile.

3.3 Trap Emission Time Constants

$$e_n = v \cdot exp(-E_t / kT)$$

Different traps have emission time constants ranging from microseconds to seconds [15,16,20]. When GPC pattern frequency is tuned near this time constant, capture occurs but emission cannot complete — net trap occupancy increases. This phenomenon is known as trap pumping.

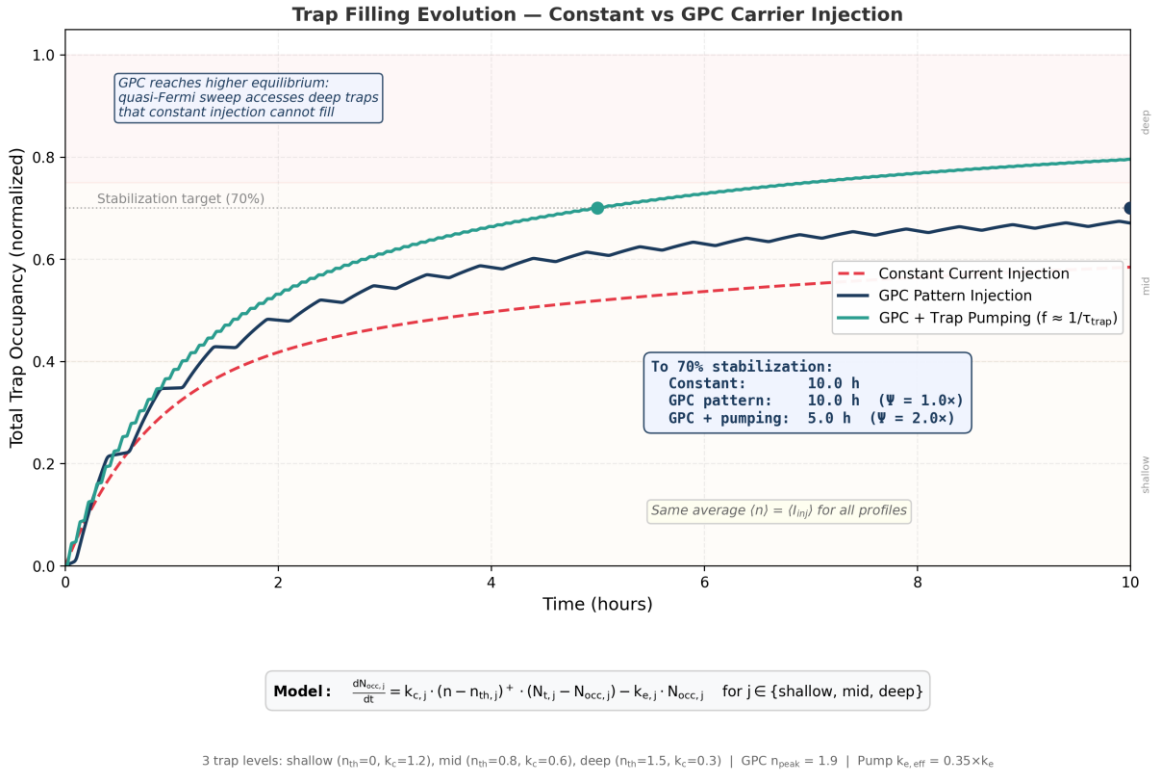

Figure 1. Multi-Level Trap Filling: Constant vs GPC Carrier Injection — Model-derived

Figure 1. Multi-level trap filling evolution: constant current vs GPC injection. GPC + trap pumping reaches stabilization target at 2.0× speed. Model-derived.

4. GPC-Based Carrier Injection Framework

4.1 From Constant Current to Pattern Current

Conventional injection: I_inj(t) = I_0 (constant). GPC injection:

$$I\_inj(t) = I\_dc + I\_ac(t)$$

where I_dc is the baseline current and I_ac(t) is a temporal structure from the GPC pattern library. Same average current is preserved: ⟨I_inj⟩ = I_0. But peak carrier density is increased: n_peak > n_dc.

4.2 Mechanism 1 — Peak Carrier Density (Dominant)

Since SRH capture rate R_c ∝ n, the n_peak created by GPC directly increases capture rate. Average capture rate:

$$\langle R\_c \rangle = \sigma \cdot v\_th \cdot \langle n(t) \rangle + \text{nonlinear terms } (\propto n\_peak^2)$$

4.3 Mechanism 2 — Quasi-Fermi Level Oscillation

$$E\_Fn = E\_C - kT \cdot \ln(N\_C / n)$$

As n increases, E_Fn rises; as it decreases, E_Fn drops. During GPC pattern, E_Fn oscillates periodically, activating traps at different energy levels sequentially. This mechanism is particularly important for amorphous silicon, perovskite, and interface traps.

4.4 Mechanism 3 — Trap Pumping

Regime	Condition	Effect
Low frequency	f ≪ 1/τ_trap	Only n_peak effect
Mid frequency (optimum)	f ≈ 1/τ_trap	Trap pumping — net occupancy increases
High frequency	f ≫ 1/τ_trap	Resembles constant current

4.5 Activation Acceleration Factor

$$\Psi_{GP,PV} = t_{act,ref} / t_{act,GP}$$

Expected range: Ψ_GP,PV = 1.5–3.0 (dependent on chemistry and trap distribution).

The acceleration factor depends on the relative contributions of the three mechanisms. For crystalline silicon with dominant B-O defects, Mechanism 1 (peak carrier density) and Mechanism 3 (trap pumping) are expected to dominate, as the B-O trap has a well-characterized emission time constant in the millisecond range [5,8,18]. The optimal GPC frequency for B-O stabilization is therefore in the 100 Hz – 1 kHz range. For amorphous silicon and perovskite technologies, where trap distributions are broader and span multiple energy levels, Mechanism 2 (quasi-Fermi level oscillation) becomes more significant, and swept-frequency or multi-tone GPC patterns may provide additional benefit [15,16].

The acceleration factor is bounded from above by the ratio of peak to average carrier density achievable without exceeding the cell's maximum injection level. Excessive carrier injection can cause local heating, increased Auger recombination, or, in the case of perovskite cells, ion migration that degrades rather than stabilizes the interface [2]. The GPC framework addresses this through the same stress index methodology used in battery applications: S_act = (n_peak/n_ref)^α × f_T × f_mode, where α is the technology-specific stress exponent and f_T captures thermal sensitivity. The activation protocol operates within the constraint S_act less than S_max, ensuring that acceleration does not come at the cost of irreversible damage.

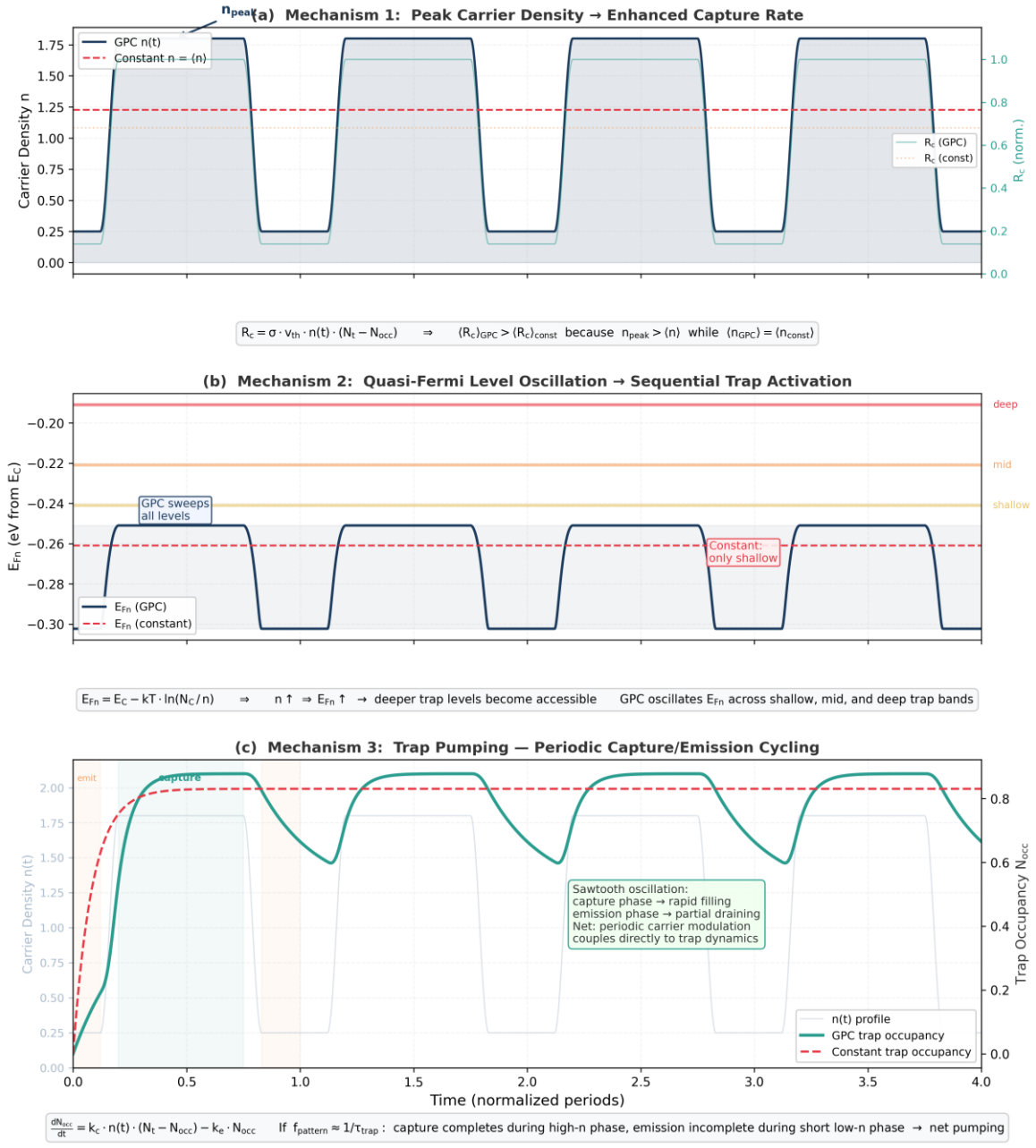

Figure 2. Three Mechanisms of GPC-Accelerated Trap Stabilization — Model-derived

Figure 2. Three mechanisms of GPC-accelerated trap stabilization: (a) peak carrier density, (b) quasi-Fermi level oscillation, (c) trap pumping. Mathematical model below each panel. Model-derived.

5. Unified Framework: Battery Formation ↔ PV Activation

Although battery formation and photovoltaic activation belong to different physical domains, both processes can be interpreted as interfacial stabilization problems driven by time-varying electrical excitation. Common dynamic form:

$$dX/dt = K_1 \cdot \Phi\_build(t) - K_2 \cdot \Phi\_harm(t)$$

Parameter	Battery Formation	PV Activation
State variable X	SEI thickness δ_SEI	Trap occupancy N_occ

Constructive driver Φ_build	Li-ion flux J_Li	Carrier density n(t)
Harmful driver Φ_harm	η_RMS, I²R, plating risk	Overheating, over-injection
Control variable	I_charge(t) pattern	I_inj(t) pattern
Acceleration factor	Ψ_GP,batt	Ψ_GP,PV

This analogy is not cosmetic. In both systems, the same mathematics applies: time-varying electrical excitation directly controls the kinetic driver of the interface or defect process. GPC is the paradigm that applies this control philosophy independently of the physical domain.

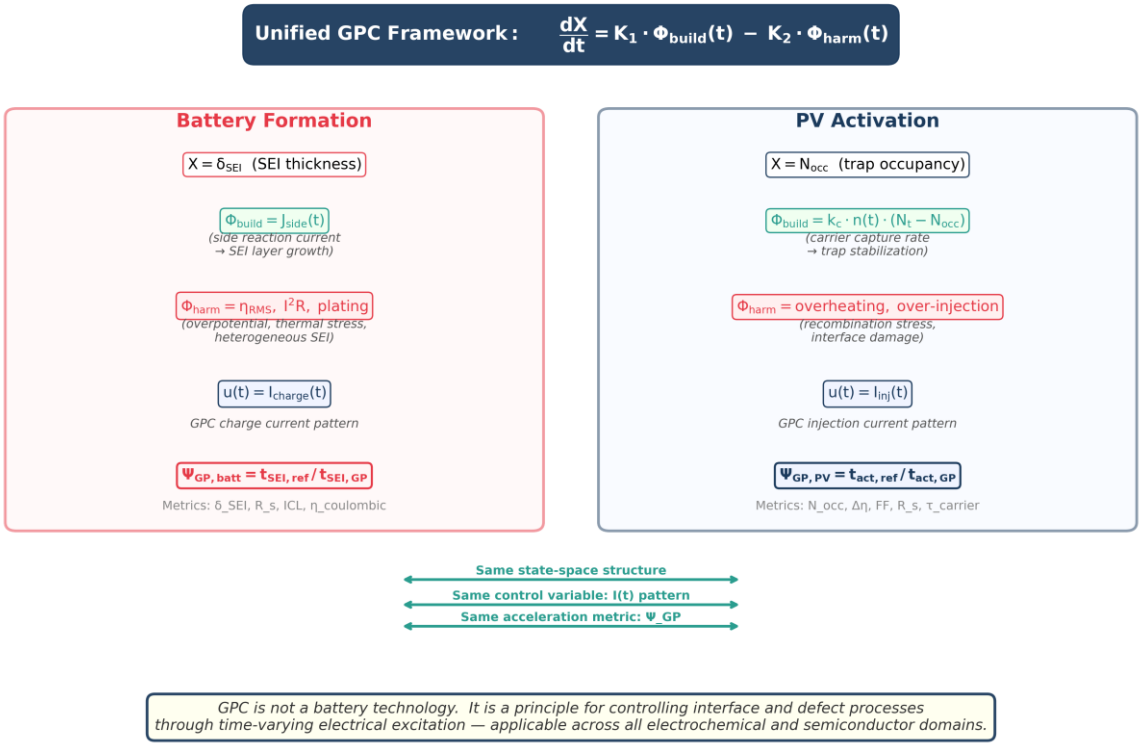

Figure 3. Unified GPC Framework: Battery Formation ↔ PV Activation Analogy

Figure 3. Unified GPC framework: battery formation ↔ PV activation analogy. Same state-space structure, same control variable, same acceleration metric.

6. Activation Metrics and Expected Outcomes

Parameter	Typical Effect	Measurement Method
Activation time	↓ 20–50%	Time to efficiency stabilization
Fill factor (FF)	↑ 0.5–1%	IV curve analysis
Efficiency stabilization	Faster	Δη time series
Series resistance R_s	Decrease	IV curve / EIS
Carrier lifetime τ	Stabilization	Photoluminescence

GPC activation does not change the maximum theoretical efficiency of PV. It does not alter fundamental semiconductor properties. It accelerates only the activation kinetics.

7. Experimental Validation Framework

Validation of GPC-based PV activation requires a proposed experimental protocol with three comparisons: constant current injection (baseline), sinusoidal-modulated GPC injection, and pulsed GPC injection. Under all three conditions, IV curve, power output, efficiency, and thermal response are measured. The activation acceleration factor is computed as Ψ_GP,PV = t_act,ref / t_act,GP.

PV cells can be directly tested in a controlled environment [17,21]. A GPC pattern generator can be integrated into any PV test laboratory alongside a standard solar simulator and IV measurement system [3,25]. All measurements are performed with equipment already present in PV manufacturing and research lines.

The proposed validation protocol consists of three parallel test groups, each containing a minimum of 10 cells from the same production batch to ensure statistical significance. Group A receives constant current injection at the baseline level I_0. Group B receives sinusoidal-modulated GPC injection with the same average current but a peak-to-average ratio of 1.5–2.0. Group C receives pulsed GPC injection with frequency tuned to the estimated dominant trap emission time constant of the specific cell technology. All three groups are maintained at the same temperature (25 ± 0.5 °C) using a temperature-controlled stage.

For each group, the following measurements are performed at regular intervals (every 30 minutes during the first 6 hours, then every 2 hours for up to 72 hours): (i) full IV curve under standard test conditions (AM1.5G, 1000 W/m², 25 °C) to extract efficiency, fill factor, open-circuit voltage, and short-circuit current; (ii) series resistance and shunt resistance from the IV curve slope analysis; (iii) photoluminescence imaging to map spatial uniformity of carrier lifetime [21]; (iv) electroluminescence imaging to detect localized defect regions. The activation endpoint is defined as the time at which efficiency change between consecutive measurements falls below 0.01% absolute for three consecutive intervals.

The primary quantitative metric is the activation acceleration factor Ψ_GP,PV = t_act,ref / t_act,GP, where t_act,ref is the time to endpoint under constant current (Group A) and t_act,GP is the time under the GPC protocol (Group B or C). Secondary metrics include the final efficiency differential Δη between groups, the fill factor improvement ΔFF, and the carrier lifetime stabilization rate measured by photoluminescence decay. For crystalline silicon cells where boron-oxygen LID is the dominant mechanism, the expected Ψ_GP,PV range is 1.5–3.0 based on the trap pumping analysis in Section 4 [4,5,9,10]. For perovskite and thin-film technologies where trap distributions are broader and quasi-Fermi level oscillation plays a larger role, Ψ_GP,PV may differ and must be characterized empirically for each technology.

8. Conclusion

PV module activation has been modeled in the literature through average injection current and temperature variables. This paper establishes that the actual driver of activation kinetics is the temporal dynamics of carrier density — n(t). GPC-based carrier injection accelerates activation through three physical mechanisms by applying a parameterized pattern current instead of constant current: peak carrier density increase, quasi-Fermi level oscillation, and trap pumping.

These mechanisms form a mathematical parallel with SEI control physics in battery formation [22,23,24]: $dX/dt = K_1 \cdot \Phi\_build(t) - K_2 \cdot \Phi\_harm(t)$. GPC is not a battery technology. It is a principle for controlling interface and defect processes through time-varying electrical excitation.

The principal quantitative predictions are: (i) activation time reduction by a factor of 1.5–3.0 ($\Psi_{GP,PV}$) relative to constant current injection at the same average current; (ii) enhanced fill factor recovery of 0.5–1% through more complete trap stabilization; (iii) faster efficiency stabilization, reducing the transient period during which module output is below nameplate rating [3,25]. These improvements are achieved without increasing the total injected energy — only the temporal structure of carrier density is modified.

The practical significance for PV manufacturing is twofold. First, accelerated activation reduces the time between module fabrication and performance certification, directly improving production throughput in manufacturing lines where activation is a bottleneck [11]. Second, the GPC approach provides a pathway to active management of LID during the activation phase, potentially converting a passive degradation process into a controlled stabilization step [6,7,10]. For crystalline silicon modules where boron-oxygen complex formation is the dominant concern, frequency-tuned GPC injection targeting the B-O trap emission time constant offers a physically motivated strategy for LID mitigation that is distinct from and potentially complementary to existing approaches such as regeneration annealing [9].

Future work will focus on experimental validation across three PV technology platforms: crystalline silicon (where B-O complexes and LID are dominant [4,5]), perovskite (where ion migration and trap redistribution govern early-life behavior), and thin-film CIGS (where interface traps at the heterojunction determine activation kinetics). The open validation framework defined in Section 7 enables any PV research laboratory to independently verify the predicted acceleration factors using standard equipment. This principle applies, starting from battery and PV, to every domain where the temporal structure of electrical excitation can direct interface or defect processes toward a targeted outcome [1].

References

[1] I. Karakoc, "Dynamic Defined Pattern Charging (DDPC)," PCT/TR2025/051176; USPTO 19/298,223. Priority: July 23, 2025.

[2] W. Shockley and H. J. Queisser, "Detailed Balance Limit of Efficiency of p-n Junction Solar Cells," J. Appl. Phys., vol. 32, no. 3, pp. 510-519, 1961.

[3] M. A. Green et al., "Solar Cell Efficiency Tables (Version 62)," Prog. Photovolt.: Res. Appl., vol. 31, pp. 651-663, 2023.

[4] T. Niewelt, J. Schon, W. Warta, S. W. Glunz, and M. C. Schubert, "Degradation of Crystalline Silicon Due to Boron-Oxygen Defects," IEEE J. Photovolt., vol. 7, no. 1, pp. 383-398, 2017.

[5] J. Schmidt and K. Bothe, "Structure and Transformation of the Metastable Boron- and Oxygen-Related Defect Center in Crystalline Silicon," Phys. Rev. B, vol. 69, p. 024107, 2004.

[6] S. W. Glunz, S. Rein, W. Warta, J. Knobloch, and W. Wettling, "Degradation of Carrier Lifetime in Cz Silicon Solar Cells," Sol. Energy Mater. Sol. Cells, vol. 65, pp. 219-229, 2001.

[7] M. Vaqueiro-Contreras et al., "Identification of the Mechanism Responsible for the Boron Oxygen Light Induced Degradation in Silicon Photovoltaic Cells," J. Appl. Phys., vol. 125, p. 185704, 2019.

[8] J. Schmidt, K. Bothe, et al., "Electronically Stimulated Degradation of Silicon Solar Cells," J. Mater. Res., vol. 21, no. 1, pp. 5-12, 2006.

[9] A. Herguth, G. Schubert, M. Kaes, and G. Hahn, "Investigations on the Long Time Behavior of the Metastable Boron-Oxygen Complex in Crystalline Silicon," Prog. Photovolt.: Res. Appl., vol. 16, pp. 135-140, 2008.

[10] B. Hallam et al., "Eliminating Light-Induced Degradation in Commercial p-Type Czochralski Silicon Solar Cells," Appl. Sci., vol. 8, no. 1, p. 10, 2018.

[11] X. Yu et al., "An Industrial Solution to Light-Induced Degradation of Crystalline Silicon Solar Cells," Front. Energy, vol. 11, pp. 107-112, 2017.

[12] J. Nelson, The Physics of Solar Cells, Imperial College Press, London, 2003.

[13] W. Shockley and W. T. Read, "Statistics of the Recombinations of Holes and Electrons," Phys. Rev., vol. 87, pp. 835-842, 1952.

[14] R. N. Hall, "Electron-Hole Recombination in Germanium," Phys. Rev., vol. 87, p. 387, 1952.

[15] S. M. Sze and K. K. Ng, Physics of Semiconductor Devices, 3rd ed., Wiley, 2007.

[16] D. K. Schroder, Semiconductor Material and Device Characterization, 3rd ed., Wiley, 2006.

[17] A. Luque and S. Hegedus, Handbook of Photovoltaic Science and Engineering, 2nd ed., Wiley, 2011.

[18] K. Bothe, R. Sinton, and J. Schmidt, "Fundamental Boron-Oxygen-Related Carrier Lifetime Limit in Mono- and Multicrystalline Silicon," Prog. Photovolt.: Res. Appl., vol. 13, pp. 287-296, 2005.

[19] D. Macdonald and L. J. Geerligs, "Recombination Activity of Interstitial Iron and Other Transition Metal Point Defects in p- and n-Type Crystalline Silicon," Appl. Phys. Lett., vol. 85, pp. 4061-4063, 2004.

[20] S. Rein, Lifetime Spectroscopy: A Method of Defect Characterization in Silicon for Photovoltaic Applications, Springer, 2005.

[21] T. Trupke et al., "Photoluminescence Imaging of Silicon Wafers," Appl. Phys. Lett., vol. 89, p. 044107, 2006.

[22] E. Peled and S. Menkin, "Review — SEI: Past, Present and Future," J. Electrochem. Soc., vol. 164, pp. A1703-A1719, 2017.

[23] F. Schomburg et al., "Lithium-Ion Battery Cell Formation: Status and Future Directions," Energy Environ. Sci., vol. 17, pp. 2686-2733, 2024.

[24] S. K. Heiskanen et al., "Generation and Evolution of the Solid Electrolyte Interphase of Lithium-Ion Batteries," Joule, vol. 3, pp. 2322-2333, 2019.

[25] M. A. Green, "The Passivated Emitter and Rear Cell (PERC): From Conception to Mass Production," Sol. Energy Mater. Sol. Cells, vol. 143, pp. 190-197, 2015.

Acknowledgments

The GPC-based PV activation protocol is protected under PCT/TR2025/051176 and USPTO 19/298,223. The author is the named inventor.

Declaration of Competing Interest

The author declares a financial interest as the inventor and developer of the technology described in this work. Ibrahim Karakoc holds the intellectual property and commercial rights to the Generated Pattern Current framework. Patent applications have been filed internationally (PCT/TR2025/051176; USPTO Application No. 19/298,223).